Whereas, continuous analysis of carbon monoxide (for conversion levels), methane (for selectively patterns) and carbon dioxide (for reaction paths analyses) are provided by the NDIR analyzers, the complete analysis of the gaseous product stream is determined by gas chromatographic analysis on an intermittant basis. A portion of the product stream from each unit is analyzed by a modified Perkin-Elmer Model 154 GC using six-foot columns of Poropak Q. Valco 10-port automatic gas-sampling valves are installed with 5-ml gas loops on each instrument. A Varian CDS 101 Data Analyzer automatically controls the sample injection and completes the peak analysis. A print-out of retention times and peak areas is provided for each peak during a run. Mole percentages can be obtained by comparison of peak areas to calibration runs of known composition. Analysis of the liquid products from the traps is accomplished by extraction of the collected samples with carbon tetrachloride and subsequent analysis of the CCl_4 layer by infrared spectroscopy. In addition, liquid samples can be injected into another GC for further analysis.

4. Task I - Work Forecast for Fifth Quarter

At this stage of the project Task I, essentially, has been completed. The only remaining assignments are the calibration of the two gas chromatographs for the C_1 to C_4 hydrocarbons. This will be completed during the next quarter, however, Task II work can proceed in the absence of these data.

B. Task V - Catalysts Preparation and Characterization

In the original proposal for this work, we emphasized the fact that the major effort in the development of Fischer-Tropsch catalysts was directed towards producing liquids, e.g., C_5^+ hydrocarbons. However, based on the work summarized by Storch, Golumbic and Anderson[1], there appears to be considerable evidence to support the belief that with the appropriate choice of catalyst and reaction conditions, the Fischer-Tropsch process could be modified to produce gaseous hydrocarbons. This work will seek to establish those necessary process variables and to develop suitable catalysts.

1. Catalyst Preparations

We have prepared a number of catalysts which may be useful to the stated objectives. These catalysts were prepared according to recipes presented in Storch's book[1]. In some cases modifications were employed to facilitate ease of preparation or to obtain a series of well characterized catalysts. Table 5 is a summary of the catalysts that have been prepared in this laboratory. Table 6 is a summary of commercial catalysts that have been obtained for evaluation in this work. A seven digit alpha numeric system is used to designate the various catalysts. (The first term identifies the major metal component, the second term refers to minor metal content, the third and fourth terms identify promoters, the fifth term refers to the support, the sixth term identifies the catalyst preparer by initials, and the last term indicates the chronological ordering of the catalysts. Whenever a quantity is missing, it is omitted from the sequence.)

Table 5 Summary of Laboratory Catalysts

Item No.	Catalyst Designation	Catalyst Composition	Comments
1	Fe-Cu-K_2O-SZ-1	100 Fe:10 Cu:1 K_2CO_3	Precipitated with Na_2CO_3
2	Fe-SZ-2	Fe	Precipitated by K_2CO_3
3	Fe-SZ-3	Fe	Precipitated by $(NH_4)_2$ CO_3 to be alkali free
4	Fe-Cu-K_2O-SZ-4	100 Fe:0.3 Cu	Precipitated by Na_2CO_3
5	Fe-Fe-Cu-K_2O-SZ-5	75 Fe^{+2}:25 Fe^{+3}:20 Cu: 1 K_2CO_3	Precipitated by Na_2CO_3 ex chlorides
6	Fe-Fe-Cu-SZ-6	75 Fe^{+2}:25 Fe^{+3}:20 Cu	Precipitated by $(NH_4)_2$ CO_3 to be alkali free
7	Fe-Cu-CaO-Kg-SZ-7	100 Fe:5 Cu:30 CaO:100 Kg	Precipitated by $(NH_4)_2$ CO_3 to be alkali free
8	Fe-Cu-CaO-Kg-SZ-8	100 Fe:5 Cu:30 CaO: 100 Kg	Precipitated by Na_2CO_3
9	Fe-K_2O-CaO-Al_2O_3-SZ-9	100 Fe: 1 K_2O:1.6 CaO: 5 Al_2O_3	Fused at 950°C for 1 hr.
10	Fe-Cu-K_2O-Dol-SZ-10	100 Fe: 5 Cu:75 Dolomite: 3 K_2CO_3	Precipitated by Na_2CO_3
11	Fe-Cu-K_2O-ZnO-SZ-11	100 Fe:5 Cu:75 ZnO: 6 K_2CO_3	Precipitated by Na_2CO_3
12	Fe-Cu-Al_2O_3-RD-1	100 Fe:10 Cu:100 Al_2O_3	Alumina impregnated
13	Fe-Cu-Al_2O_3-RD-2-Cal	100 Fe:10 Cu:100 Al_2O_3	Same as 12, but calcined at 1000°C for 1 hr.
14	Fe-Cu-Kg-RD-3	100 Fe:10 Cu:100 Kg	Precipitated by $(NH_4)_2$ CO_3
15	Fe-Cu-Kg-RD-4-Cal	100 Fe:10 Cu:100 Kg	Same as 14, but calcined at 1000°C for 1 hr.

Table 5 (Contd.)

Item No.	Catalyst Designation	Catalyst Composition	Comments
16	Fe-Cu-K_2O-RD-5	100 Fe:20 Cu:0.2 K_2CO_3	Precipitated by Na_2CO_3
17	Fe-Cu-K_2O-RD-6-Cal	100 Fe:20 Cu:0.2 K_2CO_3	Same as 16, but calcined at 1000°C for 1 hr.
18	Fe-Cu-K_2O-Kg-RD-7	100 Fe:10 Cu:0.2 K_2CO_3:100 Kg	Precipitated by Na_2CO_3 ex chlorides
19	Ni-ThO_2-Al_2O_3-RD-1	100 Ni:18 ThO_2:100 Al_2O_3	Alumina impregnated
20	Ni-ThO_2-Kg-RD-4	100 Ni:18 ThO_2:100 Kg	Precipitated by $(NH_4)_2$ CO_3
21	Ni-ThO_2-Kg-RD-6-Cal	100 Ni:18 ThO_2:100 Kg	Same as 20, but calcined at 1000°C for 1 hr.
22	Ni-ThO_2-Al_2O_3-RD-3-Cal	100 Ni:18 ThO_2:100 Al_2O_3	Same as 19, but calcined at 1000°C for 1 hr.
23	Ni-ThO_2-Kg-RD-7	100 Ni:18 ThO_2:100 Kg	Precipitated by Na_2CO_3
24	Ni-ThO_2-Kg-RD-8-Cal	100 Ni:18 ThO_2:100 Kg	Same as 23, but calcined at 1000°C for 1 hr.
25	Ni-PE-12	Unsupported Nickel	Ex carbonate
26	Ni-TB-10	Arc-Vaporized Nickel	Prepared by Dent-Bierl-arc vaporization process.
27	Ni-ThO_2-Al_2O_3-SZ-12	100 Ni:18 ThO_2:100 Al_2O_3	Co-precipitated Al_2O_3 by K_2CO_3
28	Co-ThO_2-Al_2O_3-SZ-13	100 Co:18 ThO_2:100 Al_2O_3	Co-precipitated Al_2O_3 by $(NH_4)_2$ CO_3
29	Co-ThO_2-Al_2O_3-RD-1	100 Co:18 ThO_2:100 Al_2O_3	Alunina impregnated
30	Co-ThO_2-Al_2O_3-RD-2-Cal	100 Co:18 ThO_2:100 Al_2O_3	Same as 29, but calcined at 1000°C for 1 hr.
31	Co-ThO_2-Kg-RD-3	100 Co:18 ThO_2:100 Kg	Precipitated by K_2CO_3
32	Co-ThO_2-Kg-RD-4-Cal	100 Co:18 ThO_2:100 Kg	Same as 31, but calcined at 1000°C for 1 hr.

Table 6 List of Commercial Catalysts

Item No.	Catalyst Designation	Description	Supplier
1	Ni 203T	~58% nickel on kieselguhr, 1/8"x1/8" pellets, reduced.	Calsicat
2	Ni 230T	~60% on alumina, 1/8"x1/8" pellets, reduced.	Calsicat
3	Ni-G-52	33% nickel on refractory support 3/16"x3/16", reduced.	Chemetron Corp.
4	Ni-Cu-Al_2O_3-GT312	11% Ni and 1% Cu on gamma alumina, 3/16"x1/8"	Chemetron Corp.
5	Fe-G-3A	chromium-promoted iron oxide, CO conversion catalyst, 3/8"x3/16"	Chemetron Corp.
6	Fe-G-82	triple-promoted iron oxide, ammonia synthesis catalyst, granules	Chemetron Corp.
7	Co-ZrO_2-Kg-G-67	60% cobalt, zirconium promoted supported on kieselguhr, powder	Chemetron Corp.
8	Co-Kg-G-61	60% cobalt on kieselguhr powder	Chemetron Corp.
9	Co-La-900	lanthanum cobalt oxide powder	Molycorp.
10	Fe-Mag-8	Alan Wood Magnetite	PERC, ERDA

For example, Fe-Cu-CaO-Kg-SZ-8 identifies an iron-copper catalyst promoted by calcium oxide and supported on kieselguhr which was prepared by Susan Zlotnick as her eighth catalyst. Note that many of the catalysts are repeats with minor variations in method of preparation. For example, the pair, Fe-SZ-2 and Fe-SZ-3 differ only in that the latter is alkali free. This and similar combinations will permit us to evaluate the effects of alkali and support, e.g., K_2O content and alumina versus kieselguhr, on the product distribution. We anticipate evaluating these catalysts during Task II's tenure.

The surface areas and chemical analyses of many of these catalysts were reported in the first quarterly report. While additional analyses have been completed, a further report will be deferred until the next quarterly period since we are ahead of the Task II studies. Although we are exploring currently several photometric methods for analysis of metals with particular emphasis on ease of analysis and accuracy, we will defer reporting the results of additional catalysts analyses until the next quarterly period.

C. Task II - Catalysts Screening Tests

1. Introduction

Task II represents the most important task in this research project -- the development of catalysts for the synthesis of gaseous hydrocarbons. The primary goal of this project is to alter the typical product distribution indicated by the solid lines of Figure 8 to that indicated by the dotted curve. This will be accomplished by a careful analysis of the process variables including catalyst choice, reactor temperature and pressure, and H_2/CO ratio.

Work on this task began as scheduled during the second quarterly period (Q.R. #2). To ensure safety of operation as well as facility of reactant gas blending, reactor control and product analyses, preliminary studies involving olefin hydrogenation over a thoria promoted nickel catalyst preceded the experiments involving hydrogenation of carbon monoxide. These studies proved to be a useful method of training new personnel in catalytic research.

Since the studies of Franz Fischer and Hans Tropsch during the 1920's in which they reported [2] that alkalized iron turnings at 100-150 atm of hydrogen plus carbon monoxide and at 400-500°C catalyzed the production of oxygenated and aliphatic hydrocarbons, considerable efforts have been devoted to understanding this synthesis and to improving its efficiency. Excellent reviews by Storch, Anderson and Golumbic[1] and by Greyson[3] summarize much of the earlier work in this field; recent reviews by Mills and Steffgen[4] and by Vlasenko and Yuzefovich[5] update the literature on this subject. Lee, Feldkirchner and Tajbl[6] and Vannice[7] have discussed kinetic studies over a number of catalysts. Some features which were obtained from an analysis of this vast quantity of information that have a direct bearing of the objectives of this research are summarized below.

FIGURE 8 **Product Distribution vs. Length of Hydrocarbon Chain**

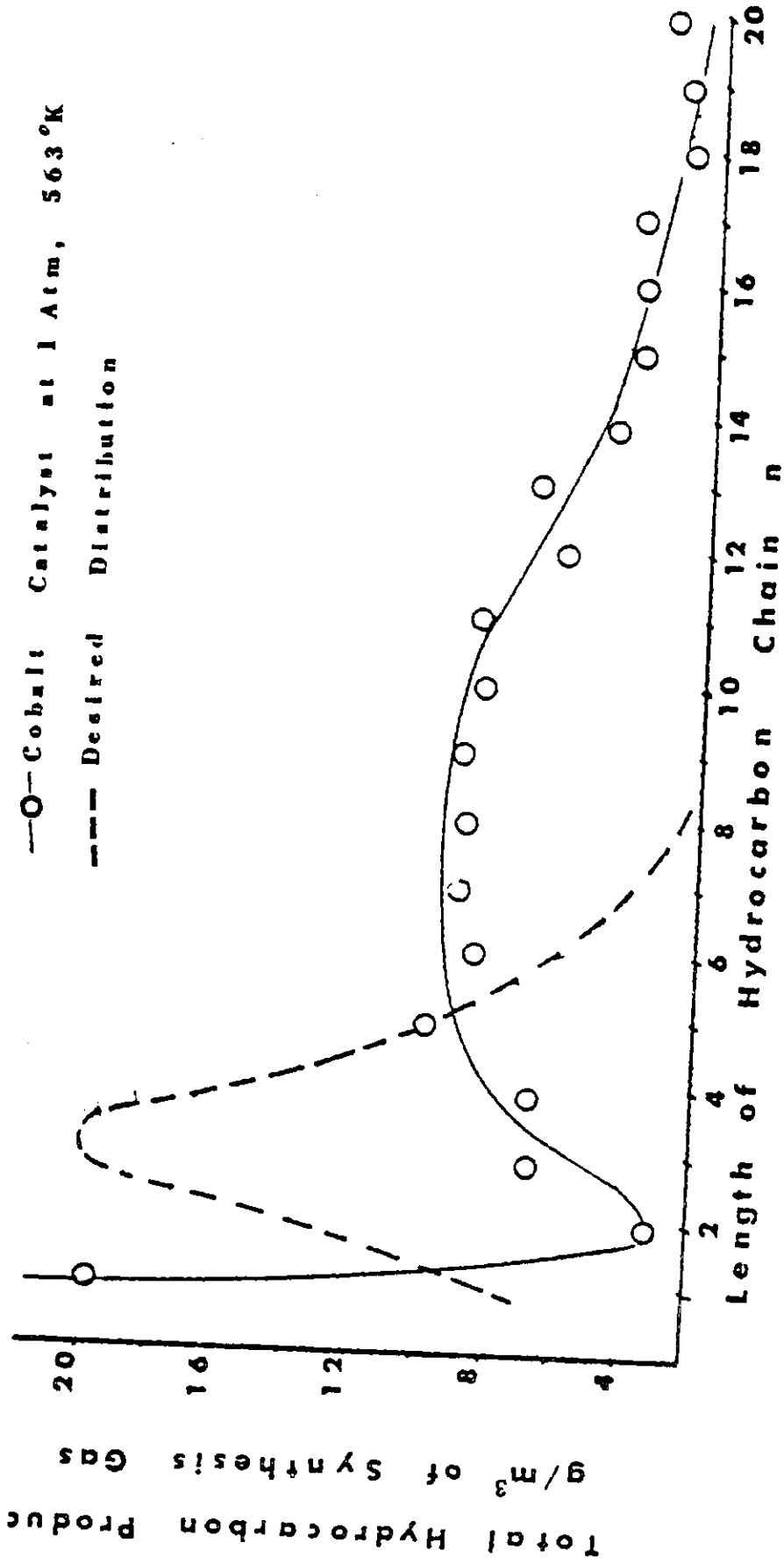

a. Pressure Effect:

(1) For iron and cobalt catalysts, the average molecular weight of hydrocarbon products increases with operating pressure up to 15 or 20 atm.

(2) For iron and cobalt catalysts, the fraction of olefins decreases slightly with increases in the operating pressure.

b. Temperature Effect:

(1) For iron catalysts, the fraction of olefins increases with the operating temperature, whereas for cobalt catalysts, the olefin fraction doesn't change much with temperature.

(2) For iron and cobalt catalysts, the average molecular weight of hydrocarbon products decreases with increasing temperatures.

c. H_2/CO Ratio Effect:

(1) For cobalt catalysts, the fraction of solid paraffins is greater with a 2:1 than with a 1:1 ratio.

(2) For iron catalysts, the fraction of light hydrocarbons (C_1-C_4) is greater with 2:1 than with a 1:1 ratio.

While there are considerably more aspects of the work reported in the literature which are important to the studies proposed for this work, the above features will serve to orient our catalyst screening program. It must be kept in mind, however, that the objectives of past Fischer-Tropsch researches focused on the production of liquid hydrocarbons from hydrogen and carbon monoxide mixtures, and, therefore, the catalysts were modified accordingly to produce the product distributions indicated by the solid line of Figure 8. Therefore, such generalizations as noted above will serve merely as guidelines for future work on this project.

2. Catalyst Screening Tests - CRU-1

Table 7 summarizes the results of ten test runs on catalyst number Fe-Cu-CaO-Kg-SZ-7. This typical Fischer-Tropsch type catalyst has the nominal composition of 100 Fe:5 Cu:30 CaO:100 kieselguhr and was prepared by the coprecipitation of the nitrates of iron, copper and calcium (slurried with kieselguhr) by the addition of a boiling solution of ammonium carbonate so as to be alkali free. Care was taken during subsequent washings to remove traces of nitrates and to ensure that the catalyst remained alkali free. A similar catalyst (Fe-Cu-CaO-Kg-SZ-8) containing potassium carbonate is scheduled for later studies to test alkali effects.

Table 7 Results of Screening Test on an Iron Catalyst[a,b]

Run No.	H_2:COHe	Space Velocity $cm^3/hr^{-1}/cm^3$ of Catalyst[c]	Temperature	Conversion Based on CO[d]	% Yield of CH_4 in Product[e]	% Yield of CO_2 in Product[e]	Comments
1[f]	2:1:7	2727	240°C	60.5%	9.0%	27%	Considerable waxes and heavy liquids formed
2	2:1:7	6080	250°C	15.6%	4.0%	5%	C_{10}^+ paraffins, alcohols and ketones
3	4:1:0	6480	240°C	19.5%	4.0%	4%	Greatest amt H_2O, alcohols, C_1-C_{16}-HC's
4	2:1:7	8850[g]	275°C	4.5%	-	-	----
5	2:1:7	8850[g]	240°C	8%	1.0%	1.0%	----
6	2:1:7	8850[g]	300°C	10%	2.0%	1.5%	Small amts alcohols; paraffins
8	3:1:6	5920	240°C	8%	5.4%	3.0%	C_2-C_6 HCs; small amt, higher HCs and oxygenated products
9	3:1:6	5920	275°C	12.5%	6.0%	6.5%	Same as #8
10	3:1:6	5920	300°C	26.4%	10.0%	2.7%	Same as #8

[a] Catalyst: 100 Fe:5 Cu:30 CaO:100 kieselguhr (~ 100 mesh size)

[b] Reactor Pressure = 100 psig; total reaction time ≈ 48 hours

[c] Total Flow Rate = 3 liters/min.

[d] Conversion (x) defined as:

$$x = \frac{([CO] + [CO_2])_{in} - ([CO] + [CO_2])_{out}}{([CO] + [CO_2])_{in}}$$

[e] Percentages based on NDIR analyses and fraction of CO in feed.

[f] 45.95 grams of catalyst used for Run #1, 21.06 grams of catalyst mixed with 42.12 grams of alumina used for all other runs.

[g] 4 liters/min. total flow rate used for this run.

Reduction of the catalyst in CRU-1's fixed-bed reactor was achieved in hydrogen at 20 psig and 450°C at a space velocity of 800 hr^{-1} for two days. Following reduction, the catalyst was cooled to 150°C under a hydrogen pressure of 40 psig. Synthesis was started at this temperature by stepwise increasing the carbon monoxide and helium pressures over a six-hour period until the final desired composition was achieved. This conditioning period is similar to that of Dry and coworkers[8] to stabilize iron catalysts.

The initial run in this series was used to train the research associate in the manipulation of a Fischer-Tropsch reactor. Details of the performance during that run were described in detail in Q.R. #3. The most important result of this run was the demonstration of the need for better heating and insulation of the reactor exit lines and for more convenient operation. Modifications resulted in the unit as described in Section III A.1 which greatly improved the unit.

The primary information gained from Runs 2-6 of Table 7 was an indication of the lifetime of this catalyst. The results indicated that no appreciable loss of activity occurred during the 24-48 hr. operation at a particular feed composition and space velocity. If each run was followed by a 6 hr. treatment in hydrogen at reaction temperature, additional runs could be obtained on the same catalyst. All catalysts were replaced after three runs as a matter of procedure. Runs 8-10 were used to estimate an activation energy for this catalyst. An Arrhenius plot of the data resulted in an apparent activation of 12.1 $\pm$ 1.0 Kcal/mole, a value in reasonable agreement to that obtained by Dry and coworkers[8] for similar iron-based F-T catalysts. This series of runs also indicated increased temperatures caused a shift to higher hydrocarbon products with methane showing the greatest increase in yield as the temperature was increased from 240°C to 300°C. Space velocity also appears to have an effect on the methane selectivity. It will be more interesting to compare these trends for other iron catalysts which have different levels of copper and/or K_2O present. These will be investigated during the second year of the project.

3. Catalyst Screening Test - CRU-2

Table 8 summarizes the results of three test runs on catalyst #Co-ZrO_2-Kg-G-67 that were completed during the fourth quarterly period. This was a commercial Girdler catalyst obtained from Chemetron Corporation in powder form and was listed as catalyst #7 in Table 6. After loading 36 cm^3 of the catalyst-kieselguhr mixture into the Berty reactor, reduction was achieved by passing hydrogen over the catalyst at a space velocity of 1667 hr^{-1} (1 liter/min. flow rate) for approximately 16 hours. The reduction temperature and pressure were 350°C and 20 psig, respectively.

Since these runs represented the initial operation of this unit, the emphasis was placed on the performance of the reactor with respect to temperature and pressure stability and control as well as the activity of the cobalt catalyst. According to Berty[9] the reactor should behave as a

Table 8 Summary of Screening Test on a Cobalt Catalyst[a,b]

Run No.	H_2:CO:He	Temperature	Reaction Time	Conversion Based on CO[c]	CH_4 Yield in Product[d]	Comments
1	3:1:6	300°C	38 hr.	18.5%	96.5%	Small amt of C_2; no heavy oils
2	3:1:6	350°C	23 hr.	24.1%	84.7%	Small amt of C_2; no heavy oils
3	3:1:6	300°C	30 hr.	19.9%	92.0%	Small amt of C_2; no heavy oils

[a] Catalyst: 60% cobalt in a cobalt-ZrO_2-Kieselguhr Girdler catalyst; 12.4 grams of a mixture of 70-30 catalyst and Kieselguhr used.

[b] Reactor Pressure = 100 psig; space velocity = 5000 $cm^3.hr^{-1}/cm^3$ catalyst

[c] Conversion defined as described in Table 7 based on 10% CO in feed.

[d] Yields based on fraction of CO consumed as analyzed by NDIRs.

continuous-stirred-tank reactor (CSTR) at rpms above 500. This was verified during the first run by increasing the number of revolutions of the impeller from 500 rpm to 2000 rpm. No change in carbon monoxide conversion occurred during these changes which led us to conclude that we were operating in the well-mixed, mass-transport free regime.

The results of Table 8 show that at 300°C and higher, methane was the primary product. Only trace amounts of carbon dioxide (less than 0.05%) appeared in the product stream. Gas chromatographic analyses indicated the principal remaining product was ethane. Only trace amounts of oily liquids were recovered from the traps. Carbon tetrachloride extraction of the aqueous products revealed that only very small amounts of alcoholic products were obtained.

Several additional test runs with this catalyst are scheduled during the next quarterly period.

4. Task II-Summary and Forecast for Next Quarter

As indicated above, catalyst testing is in progress with both CRUs. Ten runs have been completed on an iron-based F-T catalyst using CRU-1 and three runs have been completed using CRU-2 for a cobalt-based F-T catalyst. During the next quarter, additional tests will be undertaken with the emphasis on establishing possible generalizations for these catalysts.

D. Background Work for Task IV - Mechanistic Studies

The objective of this task is to obtain a fundamental understanding of the hydrogenation of carbon monoxide reaction. As noted earlier, mixtures of hydrogen and carbon monoxide react to form methane under one set of conditions (methanation) or higher hydrocarbons (alkanes, olefins and alcohols) -- the Fischer-Tropsch synthesis under another set of conditions. Since the catalysts are similar in many respects, the initial reaction intermediates, i.e. similar reaction mechanisms, must be common to both systems. Therefore, studies involving the characterization of reaction intermediates and surface species should be useful in understanding both reaction systems. Such studies, therefore, must involve techniques which permit the elucidation of relevant surface species. The coupling of infrared spectroscopic techniques with traditional mechanistic studies offers the greatest potential for providing the needed information. Techniques are being developed to facilitate such studies for both supported and unsupported metal catalysts under this task.

To date the major effort has been devoted to developing a technique to study unsupported metal catalysts by infrared spectroscopy. Since the details of this aerosol-bed technique for a nickel catalyst were reported in the first quarterly report, we will summarize work accomplished to date and indicate what future experiments are planned. A quick review of the technique might prove informative to begin.

1. A System for Studies of Nickel Aerosols in the Infrared

Since nickel is the most effective methanation catalyst, we have initiated our studies using this material. Briefly, the aerosol-bed technique involves generation of the catalyst by arc-vaporization techniques, gas-phase transfer of the aerosol to a long-path-length infrared cell where observations of surface reactions are made, and removal of the aerosol from the system by electrostatic precipitation. Arc vaporization, which is the most sophisticated of the several unit operations involved in this process, is employed as a means of generating a clean metal surface of sufficiently small particle size so as to permit infrared transmission through the bed. In this process, the metal, e.g., nickel, is vaporized at temperatures in excess of 4000°K by transfer of a high intensity electrical arc to the surface of a plug of the metal which serves as the electrode for the circuit. Since the metal is well above its boiling point, vaporization occurs at a rate proportional to the amount of heat transferred to the surface. Hence, a dense gas of metal atoms is produced. In this case these nickel atoms or atom-clusters are rapidly quenched within the vaporization chamber, and are swept through the system by the helium carrier gas. As the nickel aerosol emerges from the vaporization chamber, it passes through two heat exchangers where its temperature is adjusted as desired. The aerosol then passes into a 40 meter Wilkes long-path-length IR cell which is modified to retard deposition of the nickel particles on the mirror surfaces. Because nickel in such finely divided states represents a potential health and safety hazard, the aerosol is cleaned by passage through two electrostatic precipitators in parallel before venting the gas. Adsorbate gases can be injected into the aerosol just prior to entrance to the infrared cell. Spectral observations are made first in the absence of adsorbate gases, i.e., background conditions, then in the presence of adsorbate gases, e.g., CO, H_2, CO_2, or mixtures of these gases. An equivalent concentration of adsorbate gases in the reference beam of the Beckmann IR 12 infrared spectrophotometer used for these studies permits compensation for the gas phase effects. Thus, the difference between these two spectra represents the spectrum of adsorbed species, assuming of course that the background remains constant over this period. In this manner, a number of mechanistic studies will be conducted with the objective of characterizing the reaction intermediates at the surface of the catalyst.

This system has several advantages and disadvantages associated with it. Among its advantages is the removal of the catalyst support and consequently the opportunity to observe low frequency infrared vibrations, typically in the region where surface-to-adsorbates bonds are expected to absorb. These observations would be unobtainable otherwise. Because of the manner of operation which is essentially plug flow through the reactor, one is always observing a fresh surface. This surface may contain adsorbed species depending upon whether or not adsorbate gases were introduced into the aerosol stream. This means that a re-examination of the catalyst in the manner associated with pressed-disk IR samples is not permissible. This places a stringent requirement on the rate of aerosol generation -- it must be constant, and on the particle size distribution in the aerosol -- it too must be constant. Tests of the generation rate during two-hour periods of operation showed that the rate of aerosol generation varies by less than 5 percent over this period.

To date, this project has evolved to the stage where all of the earlier problems associated with removing 16-kilowatts of heat from the 2-liter vaporization chamber have been solved. As a result, we can generate aerosol routinely for any desired period. We have noted, however, that during several prolonged runs (2 to 3 hours of aerosol generation) the operating characteristics of the torch changed noticeably. The effect of these slight changes have been to produce drastic changes in the background spectrum. The overall effect is to produce a poor quality spectrum which makes interpretation difficult if not impossible. We have traced the source of these problems to uncontrollable oscillations in the current supplied by the two welding machines which operate the plasma torch. Since we have been able to establish a strong correlation between the operating current level and the aerosol generation rates, we currently are exploring methods to exercise greater control over this behavior. A complete analysis of the system's operating characteristics is in progress. While these aerosol fluctuations has limited infrared studies, it has not prevented us from characterizing the catalytic properties of the aerosol. These are described in the next section.

2. Physical Characterization of the Aerosol Particles

Physical characterization consisted of electron microscope examination of the particles and surface area measurements using physical adsorption of argon at liquid nitrogen temperature (77°K). The surface area measurements were reported in the second quarterly report and are summarized in Figure 9 as a function of the generation rate of the aerosol. These data are the results of several experiments obtained at a high torch-gas flow rate (60 SCFH, Θ) and at a low torch-gas flow rate (29 SCFH, Δ), and they suggest a means of producing a range of surface areas of unsupported nickel powders by this technique.

The Debye-Scherrer electron diffraction pattern was obtained from a sample of material which had been exposed to the atmosphere for several months. The sample still retained its typical intense black color, indicating it was not completely transformed to nickel oxide which is grey in color. However, the electron diffraction pattern definitely indicated the presence of nickel oxide. This is illustrated by Table 9 where the first eight rings in the pattern are assigned to line numbers (corresponding to lattice planes). The measured interplanar spacings were calculated from the radius of the rings.

Figures 10, 11 and 12 are electron micrographs of the nickel aerosol powder during this same generation run. The BET surface area of this material was 44.2 m^2/g which is equivalent to a spherical diameter of 153 Å. Figure 10 which has a magnification of 25,000X (1 cm = 0.4 microns) indicates that the particles cluster in a "tree branch" configuration with an approximate size of 1-2 microns per aggregate (longest length). This will be detrimental to infrared studies of the aerosol. Figure 11 represents an 8-fold magnification (1 cm = 500 Å) of this same sample. Here the individual particles can be observed to have a size close to that predicted by the BET measurements. (No statistical analysis was employed to confirm this.) This material was collected by a point-to-plane electrostatic precipitation (E[illegible]) technique which directly sampled the nickel aerosol.

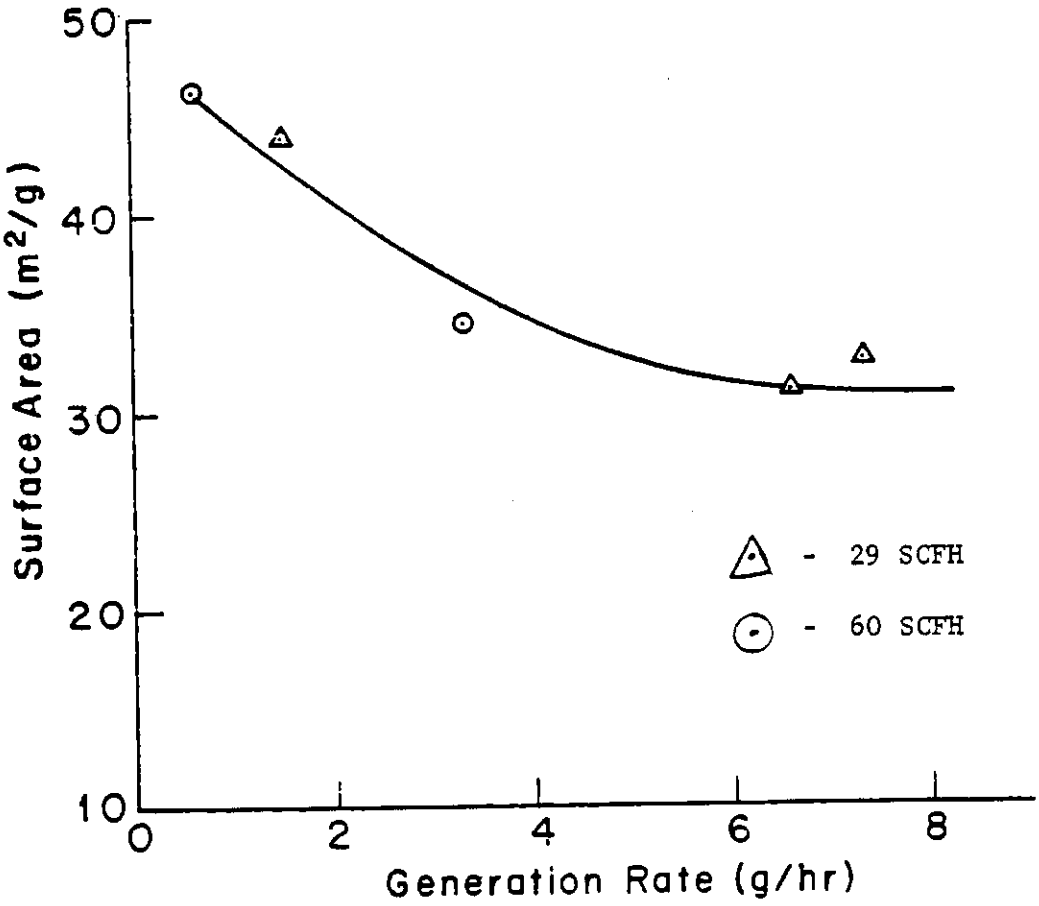

FIG. 9 SURFACE AREA VS. GENERATION RATE

Table 9 Debye Scherrer Electron Diffraction Data[d]

Line No.[a]	Interplanar Spacing Calc. NiO[b]	Interplanar Spacing (Measured)	Interplanar Spacing Calc. Ni[c]	Interplanar Spacing (Measured)
1	4.20			
2	2.97	3.17		
3	2.42		2.03	
4	2.10		1.76	1.77
5	1.88			
6	1.71			
7	1.59			
8	1.48	1.51	1.25	
9	1.40			
10	1.33			
11	1.27	1.28	1.06	1.08
12	1.21		1.02	
13	1.16			
14	1.12			
15	1.08	1.08		
16	1.05		0.881	.881
17	1.02			
18	0.99			
19	0.96		0.808	.804
20	0.94	.92	0.788	

---

[a] $N = (h^2 + k^2 + \ell^2)$

[b] $d = 3.524\ N^{-1/2}$ NiO is simple cubic

[c] $d = 4.195\ N^{-1/2}$ Ni is face centered cubic and only line numbers corresponding to this structure are tabulated

[d] All spacing in Angstrom units.

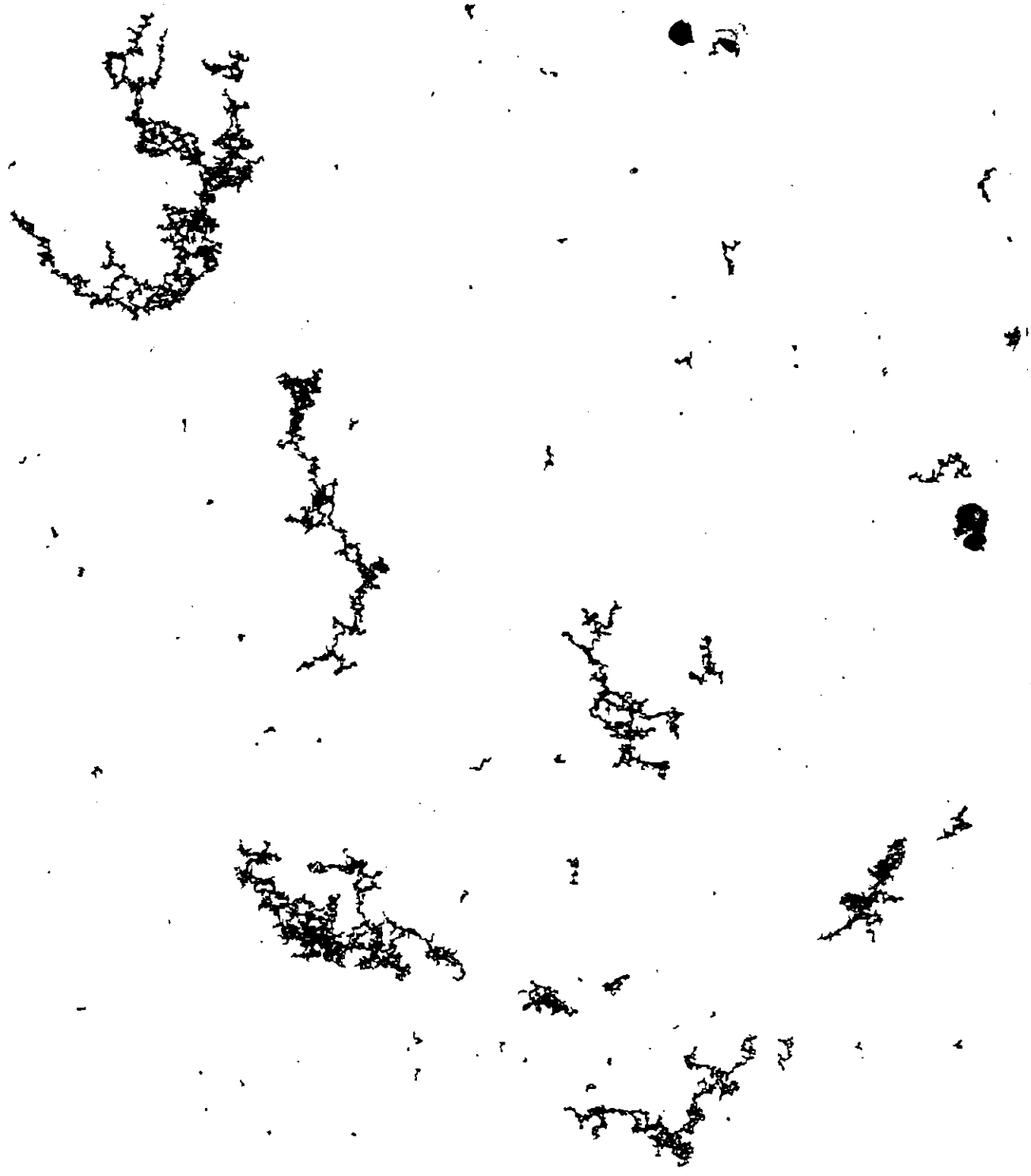

Figure 10 Electron Micrograph of Particles Collected by P-T-P Electrostatic Precipitation Magnification 25,000X

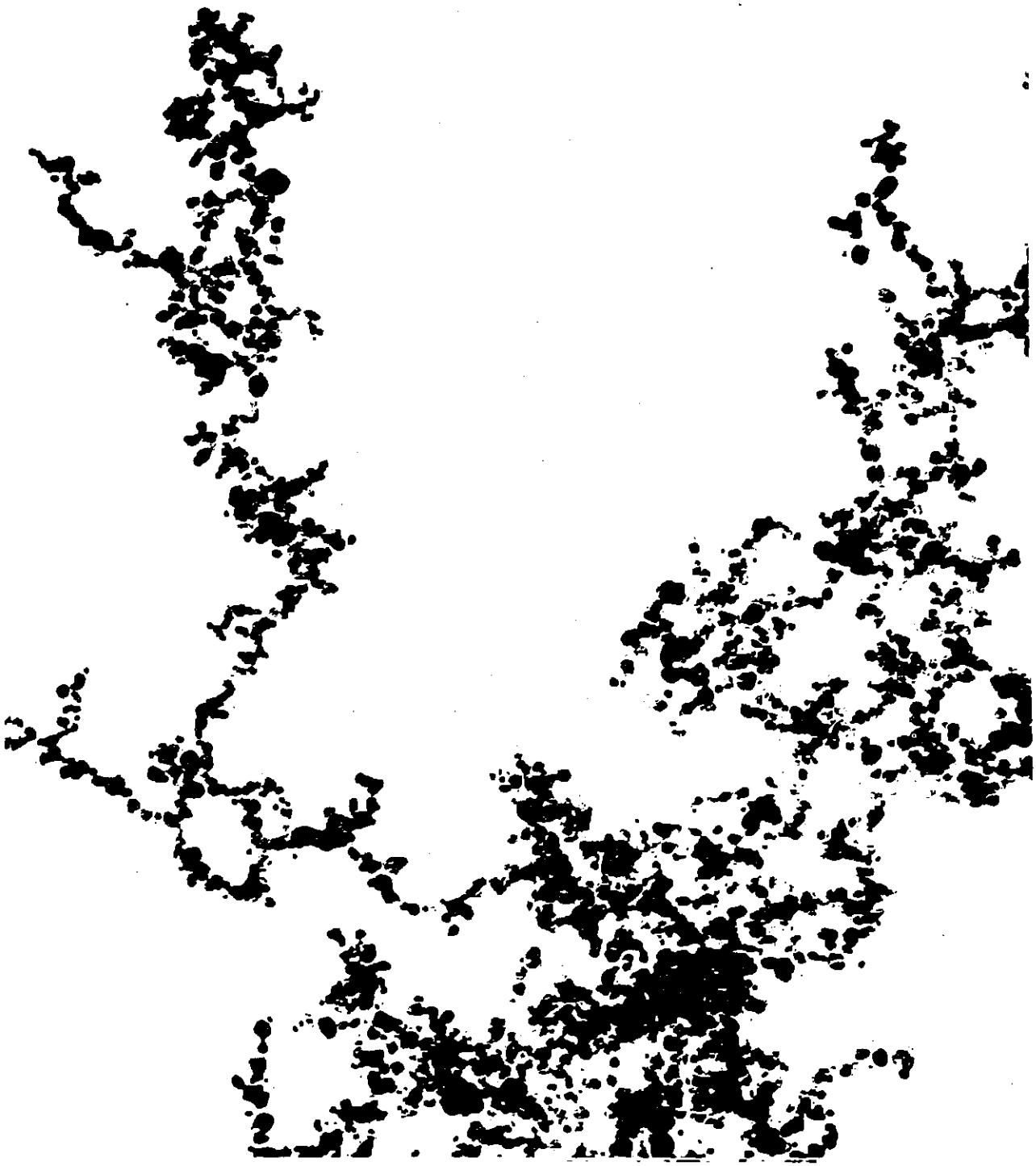

Figure 11 Electron Micrograph of Particles Collected by P-T-P Electrostatic Precipitation Magnification 200,000X

Figure 12 Electron Micrograph of Particles Collected by Forced Coagulation Magnification 200,000X

On the other hand, Figure 12 which also has a magnification of 200,000X (1 cm = 500 Å) was collected (during the same run) on a "Millipore membrane" (Millipore Co.) by drawing the aerosol through the membrane with the aid of a vacuum pump. The micrograph shows that this "forced" coagulation method produces layers of the material which must be fractured into pieces, but the sample features are similar to the P-T-P sample. Both figures show that there is significant necking between individual particles, thus indicating at least some growth by coagulation. This coagulation probably occurs during the very early stages of particle generation.

3. Catalytic Hydrogenation Studies - Review

We reported earlier that the catalytic activity of the aerosol generated nickel powder had been studied by ethylene hydrogenation at room temperature. Analysis of the data showed that this nickel is quite active catalytically. To assess how active the catalyst actually was for this reaction, a review of the literature concerning ethylene hydrogenation over nickel was undertaken. The essential aspects of that review have been completed and will be discussed as it relates to the nickel aerosol catalysts.

Catalysis does not exist without chemisorption of at least one of the reactants. It is therefore feasible that the following chemical interactions may be important to the understanding of the ethylene hydrogenation reaction over nickel: hydrogen adsorption, ethylene adsorption, ethane adsorption, hydrogen exchange reaction (H_2 in gas phase exchanges with surface hydrogen), ethylene exchange (hydrogen in the ethylene exchanges with surface hydrogen), ethane exchange (hydrogen in the ethane exchanges with surface hydrogen), self-hydrogenation, and finally the formation of stable surface complexes, "acetylenic residues." Reversibility of any of the above is also important.

Hydrogen adsorption on nickel has been investigated by many techniques -- direct adsorption measurements[10,11], and paramagnetic[12] measurements appear to be the most reliable in terms of their information content. Using paramagnetic techniques, Selwood reported that two electrons from the metal are involved with each molecule of hydrogen adsorbed, at least for fast chemisorption. This is interpreted to mean <u>atomic adsorption</u>. (There is a second (type II) chemisorption of hydrogen on nickel, but it is of no consequence here since it is very slow relative to the hydrogenation reaction.) These magnetic measurements agree with the conclusions which Beeck[10] arrived at by comparison of carbon monoxide and hydrogen adsorption. However, there are differences between the studies in terms of the percentage of the hydrogen which is retained irreversibly by the surface. Selwood reports 30% to 50% irreversibly adsorbed hydrogen, whereas Beeck reports 80% and Richardson[13] reports 20%. While the differences may be due to different catalyst pretreatments, its importance to understanding ethylene hydrogenation has been emphasized.

Richardson's data indicate that at least a portion of the irreversible sites are the ones responsible for irreversible ethylene adsorption. While his work does not completely rule out hydrogenation from occurring on reversible hydrogen adsorption sites, it does demonstrate that at 25°C, the hydrogenation reaction proceeds with extreme rapidity on all irreversible hydrogen adsorption sites. At 250°C, Richardson's data indicate that his nickel surfaces are completely covered with carbon having a low hydrogen content. Selwood[14] indicates that carbon uptakes far in excess of a monolayer can occur. This is dramatic evidence in view of the fact that Jenkins and Rideal[15] carbonized their surfaces in the presence of ethylene at 300°C to achieve a stable surface. They reported that approximately 78% of their surface was covered by "acetylenic residues." Their "bare" surface was measured by hydrogen uptake at -183°C and approximately 5×10^{-3} mm Hg. However, Eischens[16] used infrared techniques to show that acetylenic species formed under these conditions reversibly chemisorbs hydrogen even at room temperature and pressures as low as 10^{-3} mm Hg. The enhancement of this effect at low temperatures could account for the results observed by Jenkins and Rideal. This strongly suggests that for their catalysts the hydrogenation reaction must have been occurring on the carbonized surface; this would account for their considerably lower rate constants in comparison to those of Beeck[10]. It should be pointed out that Selwood[12] has reported that at 0°C dissociative adsorption of ethylene (to give acetylenic residues) is inhibited -- only two electrons per molecule of ethylene adsorbed are involved. This is indicative of associative adsorption[17]. Since much of Beeck's work was done on nickel films at 0°C, it would appear that this choice of temperatures insures that he was observing a large amount of catalysis by the nickel surface rather than by a carbonized surface which most likely occurred during the studies of Jenkins and Rideal[15]. These latter authors also reported a decay in their initial rate as a function of the exposure to ethylene. However, their highest value of a rate constant still does not approach that of Beeck.

Infrared work by Eischens and Pliskin[16] shows infrared spectral bands associated with adsorption of ethylene and ethane on nickel. There is a great deal of debate as to how the bands should be assigned[18]. But it is interesting to note the same set of bands are observed no matter what the initial conditions, and no matter whether it is ethylene or ethane. It is also noteworthy that all the infrared work has been done at room temperature or above. This is the range Jenkins and Rideal, and Beeck saw dissociative adsorption and self-hydrogenation. Eischens and Pliskin observed a change in spectrum of ethylene adsorbed on surface pretreated with hydrogen when again exposed to hydrogen, but the spectrum did not disappear with time, indicating it was not active in the hydrogenation reaction. The fact that the same set of bands is observed in the stretching region of the infrared may be indicative of the fact that the products of the dissociative adsorption of ethylene and ethane are the same kind, but their concentrations are different with varying treatment of the surface. None of these species appears to be removed easily by hydrogen and, therefore, cannot be an intermediate in ethylene hydrogenation reaction.

Schuit and coworkers[19] indicate that the H_2-D_2 exchange reaction goes very rapidly at 20°C and practically all of the deuterium preadsorbed at -195°C is utilized in forming an equilibrium D_2, H_2, HD gas phase. Because of their severe pretreatment (16 hr @ 500°C) they may have little or no irreversible hydrogen adsorption which would suggest that the reaction goes over reversible hydrogen adsorption sites. Selwood has suggested that the H_2-D_2 exchange reaction apparently occurs over carbonized surfaces[14].

Several more facts must be examined before the whole picture of hydrogenation starts to take a final form. Kemball[20] and Wilson[21] observed the products of the ethylene hydrogenation reaction at low temperatures. The results indicate a variety of deuterated ethanes (C_2H_5D-C_2D_6). These are consistent with a two-step surface mechanism first suggested by Horiuti and Polanyi[22]. This mechanism involves associatively adsorbed ethylene and adsorbed hydrogen. The problem is that Kemball, who works over metal films, sees exchange of the hydrogen in the ethylene, whereas Wilson does not. It would appear that Wilson's catalyst does not desorb ethylene from a site capable of exchange, but Kemball's surface does. Wilson worked on nickel supported by kieselguhr. An alternative explanation may be that the support has some effect on the reaction; however, it is probably due to the method of preparation. Wilson reduces his catalyst at 350°C. Schuit and Reijens[19] indicate that supported nickel-silicas required much higher temperatures for complete reduction. Several more interesting facts are worth noting: Ethane dissociative adsorption is reduced to negligible amounts by irreversibly adsorbed (preadsorbed) hydrogen[12] which means it decomposes on only the most energetic sites.

Some of the most interesting work on nickel has been done by Dalmai-Imelik and associates[23]. Well characterized surfaces were used for hydrogenation studies. The surfaces were single crystals of nickel with only one plane exposed, supported catalysts with a preferred orientation of the (111) plane and supported catalysts with random orientation. The rate constants observed in each case in the units used in this work are presented in Table 10. The temperature was 25°C and hydrogen pressure was 0.2 atm.

Table 10 Imelik's[23] Results for Hydrogenation of Ethylene

Entry	Rate Constant (cm/sec)	Type of Catalyst
1	1.97×10^{-4}	(111) oriented nickel (± 5%)
2	5.63×10^{-5}	(110) oriented nickel (± 5%)
3	~ 0	(100) oriented nickel (± 5%)
4	3.28×10^{-4}	(111) oriented nickel on a support
5	2.63×10^{-5}	no preferred orientation

The orientations do not mean the surface was a single plane; it could have been highly stepped. Also, Imelik reports "practically zero conversion" for the (100) oriented surface. This does not mean that reaction on acetylenic residues does not happen. In order for Imelik to observe conversions similar to those on the (111) and (110) oriented faces, he would have had to wait approximately one year if the rate constants calculated for the work of Jenkins and Rideal are correct. Using auger spectroscopy he observes a thick carbon layer on (100) surface. He also observes carbon on the (111) face, but it is less tenaciously held to the surface and it is arranged so as to leave free patches for hydrogen adsorption. Imelik also demonstrates the reaction rate is independent of ethylene pressure and it is first order with respect to hydrogen, in agreement with Beeck[10].

Imelik's work tends to leave open the question of hydrogenation over acetylenic residues, but it does demonstrate that it occurs on the (100) oriented surface if at all. Since Jenkins and Rideal observed very large coverage of their surfaces by acetylenic species, it would appear that the metal films they used exposed primarily (100) faces. Beeck's films under high vacuum conditions were similar, but Beeck worked at $0^{\circ}C$. This points out that the reaction which is inhibited by low temperature is dissociative adsorption on the (100) plane of nickel. It also indicates that irreversible hydrogen adsorption which apparently occurs on the (100) face (i.e. Richardson) may only partially relate to the sites active for rapid hydrogenation at room temperature observed by Imelik.

Imelik's rate data is interesting from another viewpoint. If one assumes his support is not responsible for the increase in activity between entries 1 and 4 of Table 10, then one can assume the surface defects have a very important effect on the rate. Since he could only observe an increase in rate from his (111) oriented surface if "ledges" (high Miller index planes) are important.

This review has included a great deal of speculation as to possible conclusions that can be drawn. It was done to demonstrate what may be common threads in the reported data and also to bring out the complex and contradictory state of knowledge.

4. Ethylene Hydrogenation Results over Arc Vaporized Nickel

The experiments reported here were not obtained consistent with the approach outlined above. The systematic look at ethylene hydrogenation was done as hindsight -- after results were obtained which were both exciting and difficult to explain.

The kinetic data were gathered at $24^{\circ}C$ using a microcatalytic reactor (MCR). This MCR is of rather unique design and will be discussed below. Suffice it to say here that the reactor appears to behave as a plug-flow tubular reactor without diffusion limitations, even for very high reaction rates observed here. The sample weight in these studies is an estimate based on aerosol loading (mg of Ni/ft^3). Aerosol loading was determined using "Millipore Matched Weight Gravimetric Field Monitors." They

consist of two membrane filters whose weights are matched to within 0.0001 gram. By drawing the aerosol through both filters simultaneously, the same drying conditions are experienced by both filters. Thus, the difference in weight represents the amount of nickel aerosol deposited from a measured volume of gas. (The average of three samples is taken as the aerosol loading.) With this knowledge of aerosol loading, a known volume of aerosol is drawn through the MCR. All of the particulate material is retained in the MCR as determined by placing a Millipore filter in series with the MCR.

The weight of the sample is converted to a known surface area by gathering a second much larger sample at the same conditions as an MCR sample. The surface area of the larger sample was measured by physical adsorption of argon at liquid nitrogen temperature. Its weight is determined by difference. The surface area of the nickel aerosol used in these kinetic studies was 44 m^2/g.

Figures 13 and 14 represent the final versions of the MCR cells. Two designs gradually evolved, a metal MCR (Figure 13) and a glass MCR (Figure 14). The metal cell consists of a "Gelman Membrane Filter Holder" with "Swagelok Fittings" and "Whitey Ball Valves" (Crawford Fitting Company). Unfortunately, this metal cell was found to leak during 0-50°C thermal cycles under vacuum conditions at unpredictable times. Because of this leakage, the glass MCR was developed as shown in Figure 14. A fritted glass tube (Corning Class Company, classification ~5 μm pores) serves to retain the aerosol particles. Complete retention of the aerosol was established by placing a Millipore cell downstream of the cell and noting whether discoloration of the membrane occurred.

A glass coil is placed in series upstream of the MCR to provide temperature adjustment of the feed gases to the reactor. A "Nupro very fine metering valve-double S-series" (Crawford Fitting Company) provides flow control. Ethylene-hydrogen gas mixtures from a 5-liter storage bulb are delivered to the MCR via the BET burette bulbs of a multipurpose vacuum system. Pressure is maintained constant during a run by raising the mercury levels at a rate equal to the flow rate. A pump downstream of the reactor removes the product gases. Flow rates are determined by measuring the time required for the mercury to fill a preselected burette bulb volume.

For the kinetic runs the sampling procedure is summarized as follows: The gas mixture was drawn through a heat exchanger, the catalyst bed, the flow control valve and it was either expanded into an evacuated 1-liter bulb or it was passed to the vacuum pump. To ensure constant flow rate during collection of the GC sample, caution was exercised to ensure that the sample size was such that the pressure in the bulb never exceeded half the upstream pressure. The sample was then analyzed by GC using an alumina column in a modified Perkin Elmer Model 154 GC.

Beeck[10] has shown that the hydrogenation of ethylene over nickel catalyst is first order in hydrogen and zero order in ethylene. Assuming a plug flow model for the MCR, the differential rate expression becomes

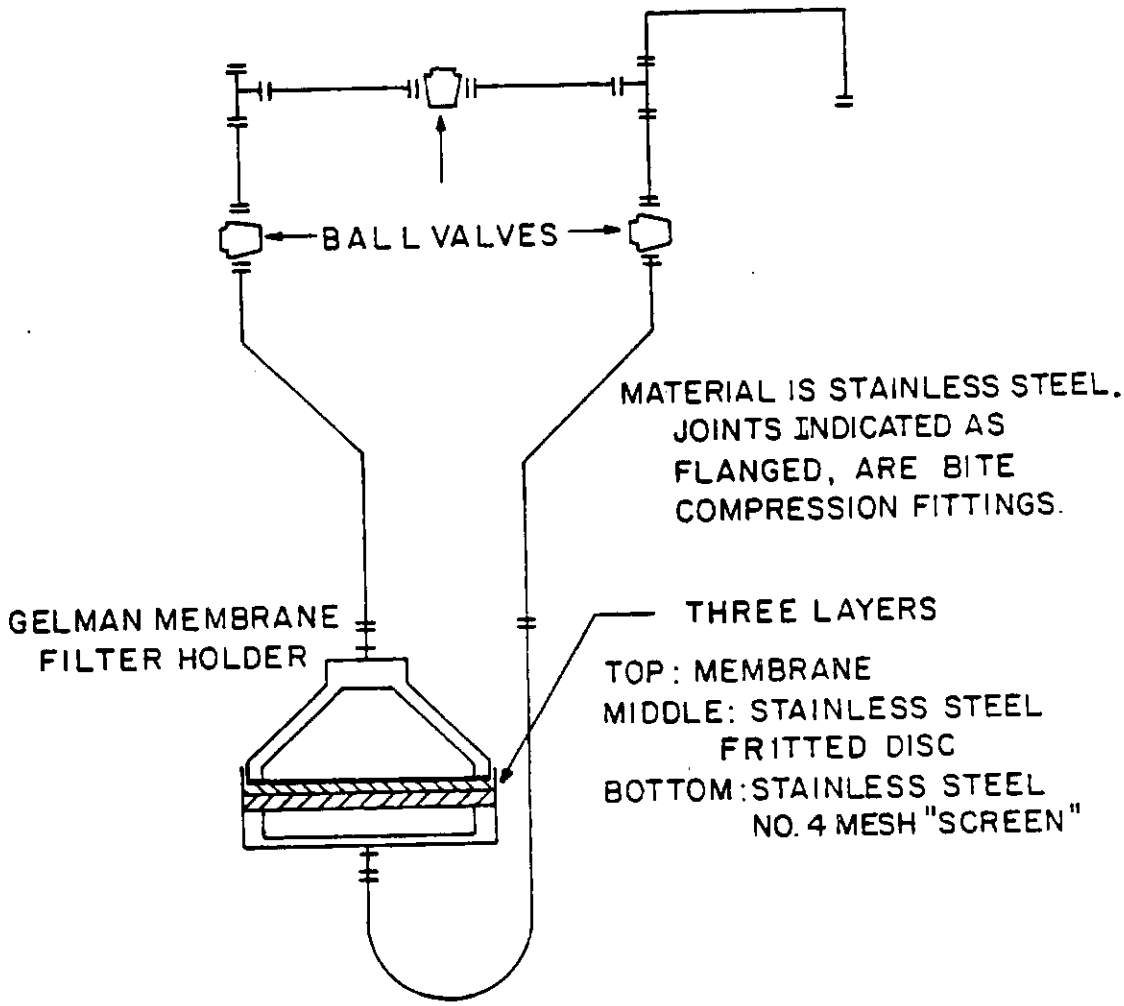

FIG. .13 MICRO-CATALYTIC REACTOR

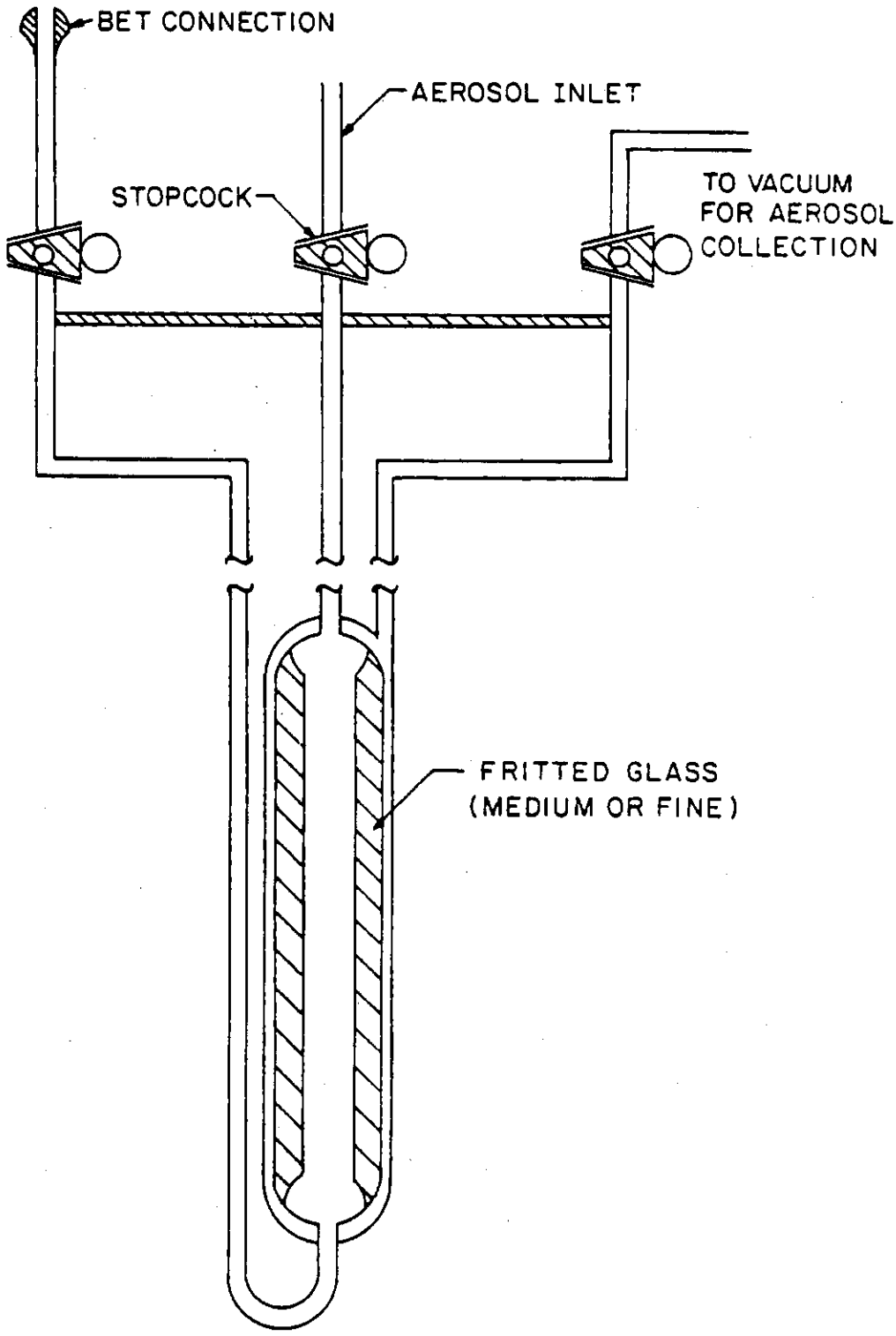

FIG. 14 AEROSOL SAMPLING CELL FOR SURFACE AERA MEASUREMENT (GLASS).

$$\frac{d}{dz} q C_e = + r_e \rho_B A Sg \qquad (1)$$

Assuming constant volumetric flow rate q, integration over the bed thickness, z, gives in terms of the extent of reaction

$$k = \frac{q}{S_T} \ln \left\{ \frac{R}{R-X} \right\} \qquad (2)$$

where r_e = reaction rate (g moles/cm^2-sec)

C_e = conc. of ethylene (g moles/cm^3)

q = volumetric flow rate (cm^3/sec)

ρ_B = bulb density of catalyst bed (g/cm^3)

A = flow area of reactor bed (cm^2)

Sg = surface area per gram of catalyst (cm^2/g)

S_T = total surface area of bed (cm^2)

R = hydrogen to ethylene ratio

k = rate constant (cm/sec)

Figure 15 and Tables 11 and 12 present the results of these studies. The data in Table 11 represent the most active catalyst tested. In fact, after an induction period (probably caused by reduction of trace quantities of oxygen in the system[15]), the conversion went to 100%. It was not possible to reduce the conversion because of limitations on the flow rate. The rate constant was greater than 3.3×10^{-4} cm/sec. It is two orders of magnitude higher than those observed by Beeck[10], and consistent with rate constants measured by Imelik[23] on oriented single crystals. This activity is substantially greater than that obtained during any other hydrogenation experiments.

The reason for this high activity may very well lie in the time sequence of events. This was the only sample which was used in a hydrogenation experiment within hours after it was taken from the arc vaporization system. No other sample was used immediately. In fact, a sample (see Table 12) was taken at the same time as the above sample and stored in vacuum (glass MCR) for four days before it was used. The rate constants observed there even after hydrogen promotion (discussed later) were an order of magnitude less. This observation seems to indicate that the surface is undergoing annealing at room temperature. This hypothesis will be rechecked during future experiments in progress.

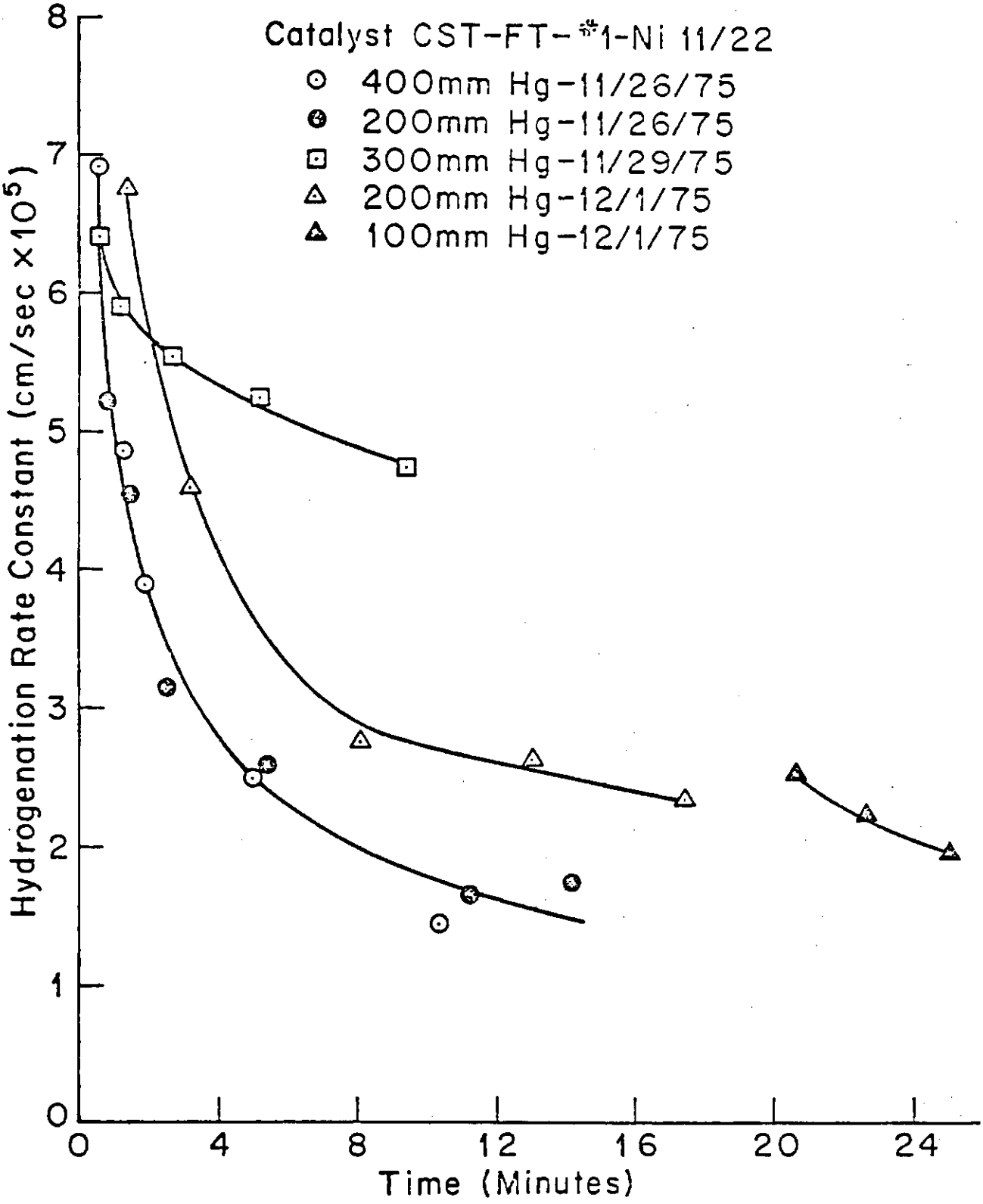

FIG. 15 HYDROGEN PROMOTION & DECAY

Table 11 Hydrogenation Data over Nickel Catalyst-Metal MCR #A[a,b,c]

Run No.	Conversion %	Flow Rate (cm^3/min)	Rate Constant (cm/sec x 10^5)	Cumulative Exposure (min)
1	2.06	93		1.82
2	99.8	93		3.39
3	100	>225	≥33.4	-

---

a Temperature: 25°C; Pressure: 400 mm Hg

b Gas Composition: H_3:C_2H_4 - 4.00:1.00 (volume ratio)

c Weight of Sample: 6.57 mg; S_T = 0.290 m^2; Sg = 44.2 m^2/g

Table 12 Hydrogenation Data over Nickel Catalyst-Glass MCR #B[a,b,c]

Run No.	Pressure mm Hg	Conversion %	Flow Rate (cm^3/min)	Rate Constant (cm/sec x 10^5)	Cumulative Exposure (min)
1	400	2.06	-		0.65
3	400	5.0	118	1.12	2.60
5	400	6.0	118	1.34	4.73
8	400	3.8	120	0.86	8.18
		H_2 Promotion @ 150 mm Hg for 5 min			
9	400	29.4	120	6.91	0.57
10	400	20.8	120	4.82	1.27
12	400	11.0	120	2.51	5.02
13	400	6.5	120	1.47	10.36
14	200	4.5	~225	1.91	12.93
15	200	4.3	164	1.33	15.19
16	200	12.21	82	1.90	18.02
17	200	5.9	108	1.20	19.94
19	200	6.1	121	1.39	23.63
		H_3 Promotion @ 150 mm Hg for 5 min			
20	200	22.4	121	5.22	0.85
21	200	19.6	121	4.55	1.48
23	200	10.9	124	2.57	5.40
24	200	7.24	119	1.63	11.23
25	200	11.5	79	1.73	14.25
		Store in Vacuum for 3 days[d]			
26	300	5.7	123	1.37	1.67
27	300	5.9	120	1.38	3.00
		H_2 Promotion @ 150 mm Hg for 5 min			
31	300	23.7	134	6.38	0.62
32	300	22.0	134	5.91	1.25
33	300	20.6	132	5.52	2.72
35	300	17.6	134	4.74	9.39
36	400	15.0	124	3.68	11.25
38	400	8.5	123	2.05	23.11

[a] Temperature: $24^{\circ}C \pm 0.6^{\circ}C$

[b] Gas Composition: $H_3:C_2H_4$ - 1.51:1.00

[c] Weight of Sample: 13.4 mg; $S_T = 0.590\ m^2$; Sg = 44.2 m^2/g

[d] After 3 days, used new gas mixture with composition $Hg:C_2H_4$ - 1.46:1.00

Table 12 summarizes the results of a catalyst collected at the same time as that described above, but which was stored for four days in vacuo in a glass cell. Figure 15 illustrates the effect of exposing the catalyst to hydrogen at 150 mm Hg pressure for five minutes at room temperature followed by successive exposures to the reaction mixture. The data points are not continuous time, but cumulative exposure time which is the sum of exposures on consecutive runs. Note that for data taken on the same day, the rate constant is independent of pressure, as it should be. The curve for data taken at a total pressure of 300 mm Hg appears to be leveling off at higher values of the rate constant than three days earlier. After an inadvertent exposure to oxygen and a reactivation cycle at 150°C, the sample levels off at a value intermediate to the previous two values. With a change in pressure and prolonged exposure (one hour), the rate constant seems to be stable at 1.43×10^{-5} cm/sec. These eradicate effects are often complained about in the literature with the result that people have unwittingly carbonized the surface to improve stability[24]. The results are obviously very dependent on the catalyst history. It appears poisoning for this catalyst is reversible by exposure to hydrogen. This was apparently not the case in the work of Jenkins and Rideal[15], but mild regeneration was done by Imelik[23] for (111) and (110) planes.

What can be speculated is that the surfaces observed here have a very high fraction of (111) or (110) planes, or else the rates should have been comparable to Jenkins and Rideal[15]. Surface annealing may be occurring and if it is, it is likely to remove defects (ledges) which are responsible for the high rate.

5. Summary and Forecast for Next Quarter

It should be pointed out that these results preceded the extensive literature review which strongly suggested that "acelytenic residues" form on the surface and inhibit the rate. These residues appear to be retarded in their formation by operation at 0°C, hence the studies described here are being repeated at the lower temperature. In addition, a strong case for structure sensitivity as demonstrated by Imelik[23] can be argued Benzene hydrogenation studies will be undertaken to explore further this concept.

IV. CONCLUSIONS

Throughout the previous sections, we have stated the work accomplished during this first year. Work is underway in Tasks #1, II, IV and V as originally scheduled. No significant milestone changes are warranted.

V. REFERENCES

[1] H.H. Storch, N. Golumbic, and R.B. Anderson, The Fischer-Tropsch and Related Syntheses; John Wiley and Sons, Inc., New York, 1951

[2] F. Fischer and H. Tropsch, Bremnstoff Chem., 4, 276-85 (1923); 5, 201-8; 217-27 (1924); 7, 97 (1926).

[3] M. Greyson, "Methanation," Catalysis, Vol. Iv (ed. P.H. Emmett), Reinhold Publishing Corp., New York, 1956, pp 473-511.

[4] G.A. Mills and F.N. Steffgen, Catalysis Reviews, 8, 189 (1973).

[5] V.M. Vlasenko and G.E. Yuzefovich, Russian Chemical Reviews, 38 (9), 728 (1969).

[6] A.L. Lee, H.L. Feldkirchner, and D.G. Tajbl, "Methanation for Coal Hydrogenation," Symposium on Hydrogen Processing of Solid and Liquid Fuels, Chicago, Amer. Chem. Soc. Division of Fuel Chemistry Preprints, 14 (4) Part I, pp 126-135 (1970).

[7] M.A. Vannice, J. Catalysis, 37, 449; 462 (1974); D.F. Ollis and M.A. Vannice, J. Catalysis, 38, 515 (1975).

[8] M.E. Dry, T. Shingles and L.J. Boshoff, J. Catalysis, 25, 99 (1972).

[9] J.M. Berty, Che. Engn. Prog., 70, 68 (1974).

[10] Beeck, O., A.E. Smith and A. Wheeler, "Catalytic Activity, Crystal Structure and Adsorptive Properties of Evaporated Metal Films," Proc. Roy. Soc., A177, 62 (1940).

[11] Schuit, G.C.A. and N.H. deBoer, "Activated Adsorption of Hydrogen on Nickel Catalysts," Recueil, 70, 1067 (1951)

[12] Selwood, P.W., Adsorption and Collective Paramagnetism, Academic Press (New York, 1962).

[13] Richardson, J.T. and H. Friedrich, "Pulsed Thermo Kinetic (PTK) Measurements: Ethylene Hydrogenation," J. Catalysis, 37, 8 (1975).

[14] Selwood, P.W., "The Chemisorption of Ethylene on Nickel-Silicas," J. Am. Chem. Soc., 83, 2853 (1961).

[15] Jenkins, G.I. and E. Rideal, "The Catalytic Hydrogenation of Ethylene at a Nickel Surface. Part I. The Chemisorption of Ethylene," J. Chem. Soc., p 2490 (1955);"Part II. The Reaction Mechanism," p 2496 (1955).

[16] Eischens, R.P. and W.A. Plishin, "The Infrared Spectra of Adsorbed Molecules," Advances in Catalysis and Related Subjects, 10, 1, Academic Press (New York, 1953).

[17] Bond, G.C., Catalysis by Metals, Academic Press (London, 1962).

[18] Little, L.H., Infrared Spectra of Adsorbed Species, Academic Press (New York, 1966).

[19] Schuit, G.C.A., N.H. deBoer, G.J.H. Dorgelo and L.L. van Reijens, "The Thermodynamics of the Adsorption of Hydrogen and the Exchange Reaction with D_2 over Metal Catalysts," W.E. Garner, ed., Chemisorption, Academic Press (New York, 1957); Schuit, G.C.A. and L.L. van Reijens, "The Structure and Activity of Metal-on-Silica Catalysts," Advances in Catalysis and Related Subjects, 10, 243, Academic Press (1953).

[20] Kenball, C., "The Deuteration and Exchange of Ethylene on Evaporated Metal Catalysts at Low Temperatures," J. Chem. Soc. (London), p 735 (1952).

[21] Wilson, J.N., J.W. Otvos, D.P. Stevenson and C.D. Wagner, "Hydrogenation of Olefins over Metals," Ind. Eng. Chem., 45, 1480 (1953).

[22] Horiuti, I. and M. Polanyi, "Exchange Reactions of Hydrogen on Metallic Catalysts," Trans. Faraday Soc., 30, 1164 (1934).

[23] Dalmai-Imelik, G. and J. Massardier, "Catalytic Activity of Single Crystal Faces: Ethylene and Benzene Hydrogenation on (111), (110) and (100), Faces of Ni Single Crystals." This paper did not bear a journal of publication. It was work conducted at Institut de Recherches sur la Catalyse; 39, boulevard du 11 November 1918; 69626-Villeurbanne, France.

[24] Wanniger, L.A. and J.M. Smith, "Kinetics of the Hydrogenation of Ethylene," Chem. Weekblad, 56, 273 (1960).

V. APPENDIX A - CONTRACT TASKS

The investigation of catalytic syntheses of gaseous hydrocarbons shall proceed according to the following tasks:

1. Task No. 1

a. Equipment and apparatus shall be assembled and integrated for the study of catalytic synthesis of hydrocarbons by means of gas chromatography and in situ high-pressure infrared spectrometry. Catalyst systems employing both fixed- and fluidized-bed mode of operation shall be provided.

b. Simultaneously with this effort the Principal Investigator shall ascertain in greater detail through discussions with catalyst manufacturers and users, the catalysts currently being employed for gaseous hydrocarbon synthesis, and the principal problems with use of such catalysts.

2. Task No. 2

Screening tests shall be developed for evaluation of catalyst formations used in synthesis of C_1-C_4 hydrocarbons. The adequacy of the tests shall be verified using catalysts known to be effective for such reactions. The tests shall be used to evaluate new catalyst preparations that offer the possibility of improved effectiveness and resistance of poisoning and sintering under the conditions of synthesis of various gaseous hydrocarbons from carbon monoxide-hydrogen mixtures.

3. Task No. 3

The most promising catalyst formulations obtained from Task 2 will be used for kinetic studies. Data obtained from the studies will be used to develop equations for predicting product yields of gaseous hydrocarbons as a function of temperature, pressure, H_2/CO ratio, and other experimental parameters. The data will also be interpreted in terms of possible reaction mechanisms, to serve as a guide for more detailed studies (Task 4).

4. Task No. 4

Studies shall be carried out on the mechanism of formation and types of reaction intermediates formed during the catalytic synthesis of gaseous hydrocarbons using the apparatus and approaches described in Task 1. In addition, catalyst poisoning and mass transfer effects will be assessed via a gas chromatographic pulsed tracer technique.

5. Task No. 5

Alternative catalyst preparation approaches will be undertaken, involving (a) the Michalko technique for imbedding catalytically active metals at a controlled depth within a catalyst pellet, and (b) development of catalyst formulations for simultaneous shift conversion and methanation.

6. Task No. 6

Tests of long-term activity, poisoning, and regeneration of catalysts shall be carried out in laboratory apparatus, and evaluations of the most promising candidates shall be conducted in a fluidized-bed reactor.

7. Task No. 7

The data obtained from Tasks 1 through 6 shall be summarized and interpreted in the final report on the contract. This final report shall include the advantages and disadvantages of each catalyst system, the economics of production of SNG and SLPG from coal-derived synthesis gas using different catalyst formulations, and recommendations for additional research in the field of catalytic synthesis of gaseous hydrocarbons.

8. Task No. 8

The Principal Investigator shall furnish consultation and advice on subject related to his expertise, at such times and places as mutually agreed upon.

These tasks shall proceed according to the following tentative schedule.